Relation between Particle Growth in Solution and Composition of Mixed Titania/Vanadium Oxide Films: Implications for Chemical Bath Deposition

Rudolf C. Hoffmann,*,† Lars P. H. Jeurgens,‡ Stefanie Wildhack,† Joachim Bill,† and Fritz Aldinger†

Max-Planck-Institut für Metallforschung and Institut für Nichtmetallische Anorganische Materialien, Universität Stuttgart, Pulvermetallurgisches Laboratorium, Heisenbergstr. 3, D-70569 Stuttgart, Germany, and Max-Planck-Institut für Metallforschung, Department Mittemeijer, Stuttgart, Germany

Received February 7, 2006. Revised Manuscript Received July 7, 2006

Composite titania/vanadium oxide thin films were prepared by chemical bath deposition. The reaction solution consisted of aqueous solutions of ammonium vanadate and a titanium peroxo complex. Deposition could be achieved on surface-oxidized silicon substrates at reaction temperatures of 333 K. The films consisted of titania as well as vanadium(IV) and (V) oxide nanoparticles. For the elucidation of the deposition mechanism the reaction solutions were investigated by dynamic light scattering to monitor the particle agglomeration in the reaction solution and UV/Vis spectroscopy to gain information about the change in chemical composition. The deposition mechanism was discussed in terms of attachment of colloidal particles. Thereby an optimum size exists for the colloids in which deposition can take place, whereas below no deposition occurs and above only the sedimentation of larger agglomerates on the surface is possible. This kinetic control leads to rather uniform films with compositions in a narrow range.

Introduction

Titania/vanadium oxide composites are of great industrial importance, whereby the material is employed in a variety of functions such as oxidation catalyst,[1,2] photocatalyst,[3,4] or ion conductor.[5,6] Accordingly, the titania/vanadium oxide composites are fabricated in a large bandwidth with respect to chemical composition (mixtures of titania as well as vanadium(V) oxide and/or vanadium(IV) oxide, which are commonly denominated TiO_2/VO_x), microstructure, morphology, and macroscopic shape. The design of the material or device thereby follows the requirements of the particular application. In the field of oxidation catalysis numerous publications deal with the grafting of titania carrier materials with vanadia surface coatings. The preparation of powders, which consist of titania and vanadium oxide particles beside each other, was also investigated. The aim is to obtain materials that show high catalytic activity and possess a large surface area.[1,2] Other applications, however, such as antimicrobial coatings,[3,4] electrodes in electrochromic devices,[5,6] and antireflective coating for solar cells[7] require titania/vanadium oxide thin films on rather planar substrates.

An alternative to the sol−gel procedures for the manufacturing of such multicomponent thin films, which were mostly used so far,[3−7] could be chemical bath deposition (CBD), which allows the deposition from aqueous solutions at low temperatures. CBD here refers to the thermohydrolysis (or "forced hydrolysis") of metal salts for the fabrication of oxidic films. For the formation of coatings or deposits by the CBD process two mechanisms are discussed in the literature, whereby mixed pathways are of course also imaginable. The first route describes the deposition in terms of the formation of colloids in the reaction solution (homogeneous nucleation) and their subsequent attachment on the substrate, which can be understood in terms of the DLVO (Derjaguin, Landau, Verwey, and Overbeck) theory. Alternatively the successive attachment of ions to the surface (heterogeneous nucleation) can lead to the growth of the coating.[8−10]

The particle attachment mechanism was investigated in detail only for the deposition of single-component films by the CBD process so far (Figure 1). The experimental findings revealed a period of time in which no film deposition occurred in the beginning. This is often referred to as induction or incubation time. Longer reaction times then lead to film growth until a limit value of thickness was reached. The deposition process was terminated when visible turbidity was observed in the solution, i.e., when larger agglomerates

* To whom correspondence should be addressed. E-mail: hoffmann@mf.mpg.de. Tel.: +49-711-6893110. Fax: +49-711-6893131.

† Max-Planck-Institut für Metallforschung and Institut für Nichtmetallische Anorganische Materialien, Universität Stuttgart

‡ Max-Planck-Institut für Metallforschung, Department Mittemeijer.

(1) Gellings, P. J.; Bouwmeester, H. J. M. *Catal. Today* **2000**, *58*, 1.
(2) Bond, G. C. *Appl. Catal., A* **1997**, *157*, 91.
(3) Fu, G.; Vary, P. S.; Lin, C. T. *J. Phys. Chem. B* **2005**, *109*, 8889.
(4) Wu, J. C. S.; Chen, C. H. *J. Photochem. Photobiol. A-Chem.* **2004**, *163*, 509.
(5) Granqvist, C. G.; Azens, A.; Isidorsson, J.; Kharrazi, M.; Kullman, L.; Lindstrom, T.; Niklasson, G. A.; Ribbing, C. G.; Ronnow, D.; Mattson, M. S.; Veszelei, M. J. *Non−Cryst. Solids* **1997**, *218*, 273.
(6) Cazzanelli, E.; Scaramuzza, N.; Strangi, G.; Versace, C.; Ceccato, R.; Cartutran, G. *Mol. Cryst. Liq. Cryst.* **2001**, *372*, 305.
(7) Ivanova, T.; Harizanova, A.; Surtchev, M.; Nenova, Z. *Sol. Energy Mater. Sol. Cells* **2003**, *76*, 591.
(8) Gao, Y.; Koumoto, K. *Cryst. Growth Des.* **2005**, *5*, 1983.
(9) Bill, J.; Hoffmann, R. C.; Fuchs, T. M.; Aldinger, F. *Z. Metallkd.* **2002**, *93*, 479.
(10) Niesen, T. P.; De Guire, M. R. *J. Electroceram.* **2001**, *6*, 169.

10.1021/cm060301t CCC: $33.50
Published on Web 08/11/2006

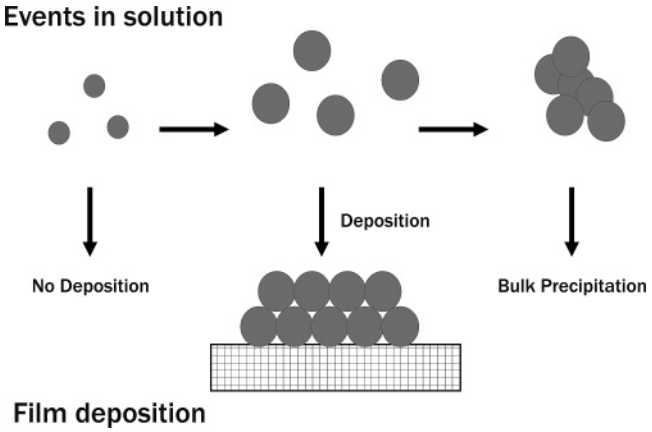

Figure 1. Schematic illustration of the different stages of particle/agglomerate formation in solution and film deposition: Single-component system TiO_2.

formed. The end of the film formation could be attributed to a competition between the growth of the film on the substrate and the colloids in the solution.[9,10]

Titania/vanadium oxide thin films were synthesized employing CBD recently, whereby the otherwise expected successive deposition of the two components was prevented by the addition of complexing agents such as peroxide[11] or fluoride[12] anions. Since the product distribution in multicomponent systems can, however, be quite complex,[13] it is an advantage that the number of the expected products in the Ti−V−O system is relatively straightforward.[14] Therefore, apart from the potential technological interest titania/vanadium oxide is a suitable model system to understand the growth mechanism of multicomponent films initiated by hydrolytic reactions.

A recent review article pointed out that conclusions for the mechanism of mineralization reactions should not be drawn from particle or film morphologies.[15] Events related to nucleation in the reaction solution must have an immediate influence on the growth process during the mineralization; however, such investigations are still rare. Methods such as small and wide angle X-ray scattering (SAXS and WAXS) provide excellent results, but might require synchrotron radiation.[16] On the other hand, dynamic light scattering (DLS) was proposed as a fast and convenient tool to investigate especially particle growth and agglomeration in mineralization processes.[17,18] The work presented here now demonstrates that UV/Vis spectroscopy is able to extend the picture provided by DLS measurements for the formation of multicomponent systems.

Experimental Section

Film Deposition. Silicon slides of 10 × 10 mm were cleaned with chloroform as well as 2-propanol and washed abundantly with distilled water afterward. Stock solutions of the titanium peroxo complex were prepared by the addition of titanium tetrachloride to an aqueous solution of hydrogen peroxide and stored in a refrigerator.[11,17] The ratio of titanium:hydrogen peroxide in the stock solution was kept at 1:2 throughout all experiments described here.

Reaction solutions were fabricated by dissolving the required amounts of ammonium vanadate in solutions of the titanium peroxo complex, 1 M hydrochloric acid (Riedel-de-Haën, Fixanal), and distilled water. For the film deposition the substrates were immersed in 10 mL aliquots of the deposition solution, covered, and placed in an oil bath at 333 K. In the case of subsequent multiple depositions, i.e., by renewing the reaction solution, substrates were cleaned by ultrasonication in water in between.

To investigate the precipitates which formed during the film deposition, powders were prepared from the reaction of 100 mL aliquots at 333 K. The powders were collected after 240 min by repeated centrifugation and washing with distilled water.

Sample Characterization. *Atomic Force Microscopy (AFM).* AFM images were recorded using a Digital Instruments Nanoscope III applying tapping mode with silicon cantilevers. The thickness of the films was determined by carefully scratching the film with a sharp needle and measuring the depth of the scratch at five locations by means of AFM.[17] The roughness was measured from five areas of 5 × 5 μm^2 size. Error bars in figures presenting these findings refer to the experimentally determined spread.

Scanning Electron Microscopy (SEM). For SEM investigations a Zeiss DSM 982 Gemini at 3.0 kV was used. Cross sections for thickness determinations were prepared by careful cleavage of the samples with an edge cutter. The thickness was measured at five locations. Error bars in figures presenting these findings refer to the experimentally determined spread.

X-ray Photoelectron Spectroscopy (XPS). XPS spectra were recorded using a Thermo VG Thetaprobe system employing monochromatic incident Al Kα radiation ($h\nu$ = 1486.68 eV; spot size 400 μm). Energy calibration and charge compensation during the measurements were carried out according to established procedures.[11] Detailed spectra of the Ti 2p, V 2p, and O 1s photoelectron lines were measured with a pass energy of 100 eV and a step size of 0.1 eV.

X-ray Diffraction (XRD). XRD diagrams were recorded using a Siemens Kristalloflex 5000 diffractometer.

Inductively-Coupled Plasma Optical Emission Spectrometry (ICP-OES). The Ti and V content of dried powders were determined with a Spectro CIROS^{CCD} photometer.

Characterization of Reaction Solution. *UV/Vis Spectroscopy.* UV/Vis transmission spectra were recorded with a Varian Cary 5000 UV−Vis−NIR spectrophotometer. Solutions were measured before as well as during the reaction (after quenching the reaction vessel in ice water) in Quartz cuvettes with 1 mm or 10 mm thickness, respectively.

Particle Size Measurements. DLS was performed with a Zetasizer Malvern 3000 HS_A. The DLS unit utilizes a HeNe laser at a wavelength of 632.8 nm with a laser power of 10 mW. The scattered light was collected at an angle of 90°. A pristine polystyrene cuvette was used for each measurement and charged with the freshly prepared reaction solution (3.5 mL) through a 20 nm size filter (Whatman, Anotop 25). Placement of the cuvettes in the holder, which used a Peltier element for maintaining the reaction temperature, is defined as $t = 0$. The reaction temperature was reached after about 3 min. Correlation functions were recorded every 30 s for 125 min or every 60 min for 250 min, respectively. Data evaluation was performed with the software supplied by the

(11) Hoffmann, R. C.; Jeurgens, L. P. H.; Wildhack, S.; Bill, J.; Aldinger, F. *Chem. Mater.* **2004**, *16*, 4199.
(12) Shyue, J. J.; De Guire, M. R. *Chem. Mater.* **2005**, *17*, 5550.
(13) Narendar, Y.; Messing, G. L. *Catal. Today* **1997**, *35*, 247.
(14) Enomoto, M. *J. Phase Equilib.* **1996**, *17*, 539.
(15) Horn, D.; Rieger, J. *Angew. Chem., Int. Ed.* **2001**, *40*, 4330.
(16) Pontoni, D.; Bolze, J.; Dingenouts, N.; Narayanan, T.; Ballauff, M. *J. Phys. Chem. B* **2003**, *107*, 5123.
(17) Hoffmann, R. C.; Bartolome, J. C.; Wildhack, S.; Jeurgens, L. P. H.; Bill, J.; Aldinger, F. *Thin Solid Films* **2005**, *478*, 164.
(18) Cölfen, H.; Schnabelegger, H.; Fischer, A.; Jentoft, F. C.; Weinberg, W.; Schlögl, R. *Langmuir* **2002**, *18*, 3500.

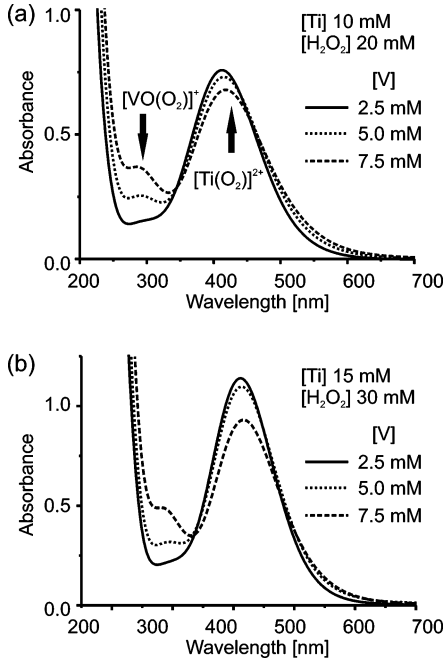

Figure 2. UV spectra of solutions prior to reaction containing (a) 10 mM Ti, 20 mM H_2O_2, 100 mM HCl or (b) 15 mM Ti, 30 mM H_2O_2, 100 mM HCl and various amounts of V (2.5, 5, and 7.5 mM, respectively).

manufacturer employing the analysis mode for monomodal samples (ISO 13321), which yields an average value for the hydrodynamic radius and the polydispersity index as a characteristic for the size distribution.

Results and Discussion

Behavior of Reaction Solution. Reaction solutions for the deposition of multicomponent systems can comprise a rather large number of parameters. Therefore, in the current investigation a variety of different compositions were checked to be at least to some extent able to assess the influence of a given parameter. Hereby, the concentrations of titanium and vanadium ions as well as hydrochloric acid were varied. As mentioned above the molar ratio of titanium: hydrogen peroxide in the stock solution (and therefore also in the deposition solutions prior to the reaction) was kept at 1:2.

The solutions showed a change in appearance during the course of the deposition experiments. The color of the solutions was red or orange-red directly after preparation (Figure 2), indicating the presence of peroxo complexes of both titanium and vanadium, which possess LMCT (ligand to metal charge transfer) bands in the UV/Vis range.[19,20]

The signal of the $Ti[(O_2)]^{2+}$ complex ion can be found at about 410 nm, whereas that at 290 nm can be attributed to $[VO(O_2)]^+$ ion. The formation of $[VO(O_2)_2]^-$ would only be expected in solutions with large excess of H_2O_2.[21,22] The reaction solutions were stable within 24 h; i.e., no apparent changes became visible. Upon heating, though, the solutions showed rapid discoloration followed in some cases by the occurrence of turbidity. These findings could be quantified by means of UV/Vis spectroscopy and DLS.

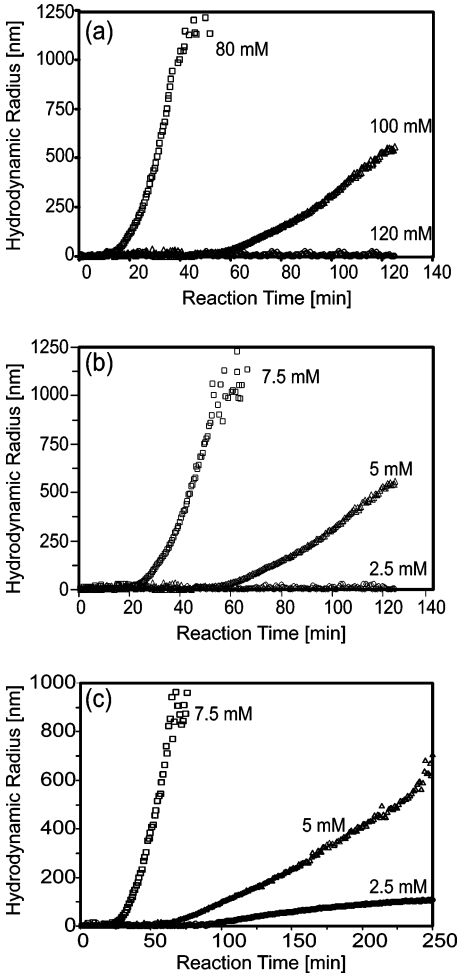

Figure 3. Particle size as measured by DLS vs time from solutions containing (a) 10 mM Ti, 20 mM H_2O_2, 5 mM V and various amounts of HCl (120, 100, and 80 mM, respectively), (b) 10 mM Ti, 20 mM H_2O_2, 100 mM HCl and various amounts of V (2.5, 5, and 7.5 mM, respectively), and (c) 15 mM Ti, 30 mM H_2O_2, 100 mM HCl and various amounts of V (2.5, 5, and 7.5 mM, respectively).

The results of the DLS measurements are presented in Figure 3, which shows the progression of the mean average size (hydrodynamic radius) of the particles as a function of reaction time.

The curves showed a typical course, which was described in detail for the deposition of titania from titanium peroxo complexes.[17] The curves started with a horizontal region in which the particle size or the particle concentration are in the range of the detection limit of the DLS instrument (<20 nm).[17,18] This induction time was then followed by a rapid increase in particle size. This increase is, however, mostly attributed to the formation of agglomerates rather than a significant growth of the size of the primary crystallites, which were previously formed in the induction period.[17,18]

A first set of measurements (Figure 3a) was carried out for solutions containing various amounts of hydrochloric acid (80, 100, and 120 mM) but with the same titanium and vanadium ion concentration (10 mM Ti and 5 mM V). The duration of the induction depended on the concentration of acid in the reaction solution; i.e., higher concentrations of acid lead to longer induction times. In the case of 120 mM

(19) Lever, A. B. P.; Gray, H. B. *Acc. Chem. Res.* **1978**, *11*, 348.
(20) Lever, A. B. P.; Ozin, G. A.; Gray, H. B. *Inorg. Chem.* **1980**, *19*, 1823.
(21) Suzuki, N.; Kuroda, R. *Mikrochim. Acta* **1987**, *2*, 47.
(22) Conte, V.; Di Furia, F.; Moro, S. *J. Mol. Catal.* **1994**, *94*, 323.

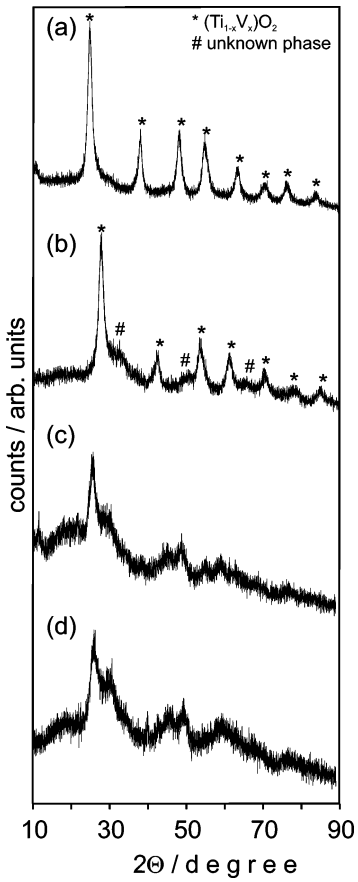

Figure 4. XRD diagrams of powders obtained after 240 min from solutions containing 15 mM Ti, 30 mM H_2O_2, 100 mM HCl and (a) 2.5 mM V, (b) 5 mM V, (c) 7.5 mM V, and (d) 10 mM V.

HCl no particle growth could be revealed in the DLS measurements. In a second set of measurements (Figure 3b) the concentration of titanium and hydrochloric acid was kept constant (10 and 100 mM, respectively) whereas the vanadium concentration was varied (2.5, 5, and 7.5 mM). In the case of 2.5 mM V no particle growth could be revealed in the DLS measurements. A third set of measurements (Figure 3c) was carried out accordingly for another titanium concentration of 15 mM.

The induction times, which can be determined in these DLS measurements, are of direct importance for the growth of films from these solutions since reaction times shorter than the induction period do not lead to the development of films.[17,18] In agreement no film growth was observed from reaction solutions containing 10 mM Ti, 5 mM V, and 120 mM HCl as well as 10 Ti, 2.5 V, and 100 mM HCl, respectively. Details about the morphology as determined in AFM and SEM measurements of films grown from the reaction solution discussed here will be presented below.

As mentioned above, larger agglomerates finally form in nearly all of the investigated reaction solutions (Figure 3). The precipitates of a set with constant Ti and HCl concentration (15 and 100 mM, respectively) as well as varying V concentration (2.5−10 mM) were collected and analyzed by means of XRD (Figure 4). The diffraction diagrams exhibit broad reflections indicating the presence of nanoparticles. An estimation of the particle size using Scherrer's formula yielded an upper limit of about 15 nm. At the lowest V concentration (Figure 4a) only the peaks of an anatase-type phase are visible. These consist presumably of solid solutions of $(Ti_{1-x}V_x)O_2$, whereby the shift of the peak positions[3,11] with respect to TiO_2 corresponds to the amount of V in the solid solution (Figure 4b). At higher V concentrations, though, further peaks occur, which however could not be assigned to a distinct titanium or vanadium oxide phase (Figures 4b−d). The peaks notably did not result from a known phase of $V_2O_5 \cdot nH_2O$.[11] The presence of amorphous V(+V) phases in TiO_2/VO_x composites was frequently observed and was attributed to the incorporation of nanosized TiO_2 into the V_2O_5 layer structure.[23,24]

Table 1. Ti and V Contents of Precipitates According to ICP/OES and Corresponding Starting Concentrations of Reaction Solutions

reaction solution		precipitate		
concentration/mmol	ratio Ti:V	wt % Ti	wt % V	ratio Ti:V
Ti 15 V 2.5 HCl 100	6.0:1.0	42.2	6.9	6.5:1.0
Ti 15 V 5 HCl 100	3.0:1.0	33.2	11.0	3.2:1.0
Ti 15 V 7.5 HCl 100	2.0:1.0	30.4	13.5	2.4:1.0
Ti 15 V 10 HCl 100	1.5:1.0	29.3	14.1	1.5:1.0

The Ti and V content of the powders were determined using ICP/OES (Table 1). The ratio of Ti:V in the precipitate follows that of the solution, indicating that the employed reaction system is able to yield films of a broad range of compositions.

As another method for the characterization of the solutions during the reaction, UV/Vis spectroscopy was employed. Here, a set of experiments for solutions with varying Ti:V ratio was carried out to determine the influence of this parameter. The change of the UV spectra with ongoing reaction time is shown in Figures 5 and 6.

A typical feature for all set of spectra for a distinct composition is the decrease of the intensity of the peak at 410 nm, which can be attributed to the $Ti[(O_2)]^{2+}$ ion, with increasing reaction time. In contrast to the spectra of the reaction solution at the start (Figure 2) no peaks of vanadium peroxo ions, neither $[VO(O_2)]^+$ nor $[VO(O_2)_2]^-$, could be detected. Instead, a sigmoidal feature with an onset of about 370−380 nm was found (with the notable exception for the set of spectra in Figure 5c), which is typical for titania or V-doped titania particles.[25,26] While the intensity of the peak of the titanium peroxo complex decreased steadily, the before-mentioned signal ascribed to titania or titania-rich particles remained almost unchanged for a certain period of time. (Due to the overlap of these effects, the exact position of the sol peak could not be determined.) Then, however, a continuous red shift of this band occurred. This could be attributed to the formation of particles containing higher amounts of vanadium. The distinction, however, whether this shift was due to the formation of V(IV), leading to $(Ti_{1-x}V_x)O_2$ solid solutions, or V(+V), in which case the precipitation of V_2O_5 would be expected, was not possible.[25] Thin layers of V_2O_5 or VO_2 on TiO_2 are known to yield UV spectra which have a gradual shift of the absorption

(23) Lee, K.; Cao, G. *J. Phys. Chem. B* **2005**, *109*, 11880.
(24) Kittaka, S.; Matsuno, K.; Tanaka, K.; Kuroda, Y.; Fukuhara, M. *J. Mater. Sci.* **2001**, *36*, 2511.
(25) Gao, X.; Wachs, I. E. *J. Phys. Chem. B* **2000**, *104*, 1261.
(26) Enache, D. I.; Bordes-Richard, E.; Ensuque, A.; Bozon-Verduraz, F. *Appl. Catal., A* **2004**, *278*, 93.

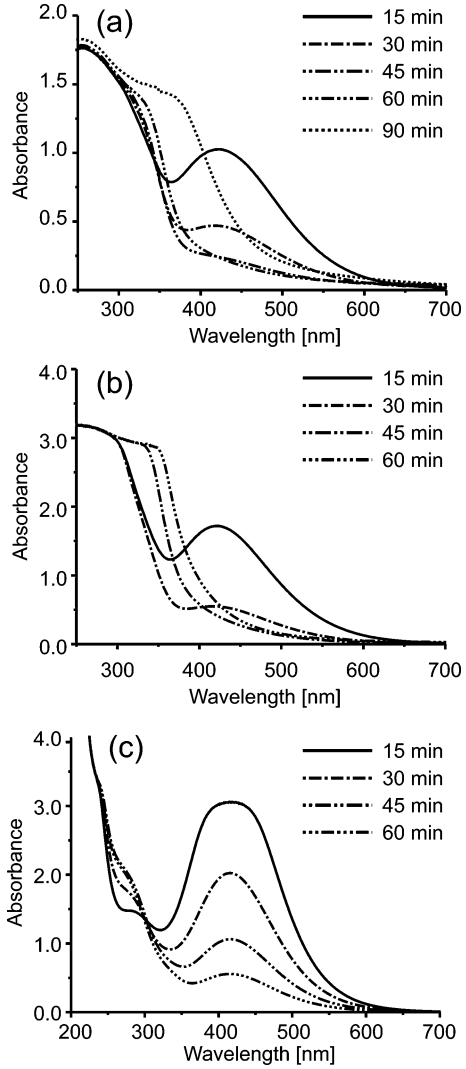

Figure 5. UV spectra of solutions after different times containing 10 mM Ti, 20 mM H_2O_2, 100 mM HCl and (a) 7.5 mM V, (b) 5 mM V, and (c) 2.5 mM V.

maximum depending on the thickness of the vanadium oxide layer, rather than distinct steps.[3,4,26]

Remarkable for the understanding of the hydrolytic reaction is that the moment at which the red shift of the sol peak occurs is (in the range of the experimental error) identical to the induction time determined from the DLS measurements. This means that the onset of rapid particle growth coincides with the occurrence of $(Ti_{1-x}V_x)O_2$ or V_2O_5 particles in the solution. Since at this point in time TiO_2 particles are already present, it could be possible that these serve as nucleation sites for the vanadium oxide phases. This is supported by the fact that a smooth shift of the UV spectra is observed, rather than distinct steps (Figures 5 and 6).

The interpretation of the UV spectra presented here does not include quantum size effects. A red shift due to particle growth of single phases (and not due to changing of the chemical composition as suggested here) cannot be fully excluded. Such an effect, however, is known to be small for TiO_2 and $(Ti_{1-x}V_x)O_2$ nanoparticles and is certainly not able to explain the shift of more than 150 nm described here.[27−29]

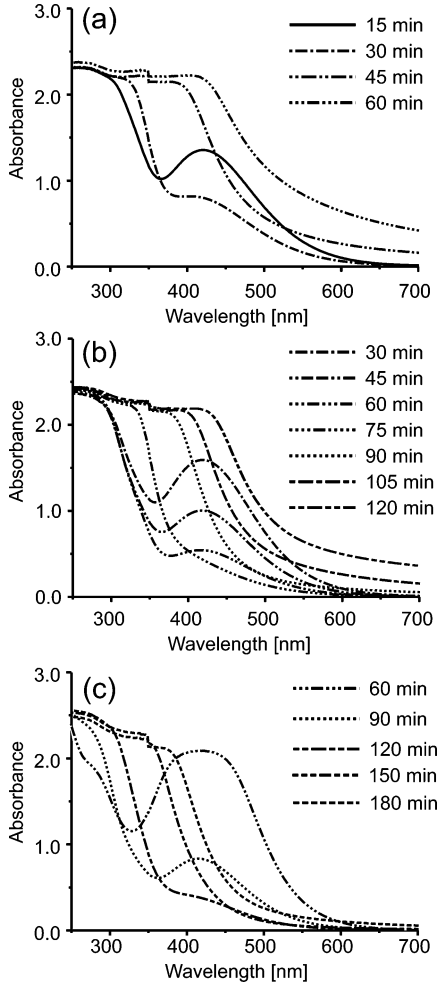

Figure 6. UV spectra of solutions after different times containing 15 mM Ti, 30 mM H_2O_2, 100 mM HCl and (a) 7.5 mM V, (b) 5 mM V, and (c) 2.5 mM V.

Characterization of Deposited Thin Films. In the following the films grown on surface oxidized silicon substrates from the previously discussed reaction solutions were investigated in more detail. The progression of thickness and roughness as a function of reaction time and renewal frequency of the solution were measured by means of AFM (Figure 7) and SEM (Figure 8). The findings, which are demonstrated here (Figure 9) for films from a solution containing 15 mM Ti, 5 mM V, and 100 mM HCl, were typical for all investigated compositions.

Below a certain induction time (here, 45−60 min in accordance with DLS measurements mentioned before) no film deposition is observed. Longer reaction times without renewal of the solution lead to thicker films only until a limit value was reached. As mentioned above, the formation of agglomerates in the reactions solution presumably leads to a competition between the growth of the film on the substrate and the colloids in the solution which finally ends the film deposition. For the manufacturing of thicker films, renewal[30] of the solution was therefore more favorable (Figure 9a). In

(27) Enright, B.; Fitzmaurice, D. *J. Phys. Chem.* **1996**, *100*, 1027.
(28) Kormann, C.; Bahnemann, D. W.; Hoffmann, M. R. *J. Phys. Chem.* **1988**, *92*, 5196.
(29) Sene, J. J.; Zeltner, W. A.; Anderson, M. A. *J. Phys. Chem. B* **2003**, *107*, 1597.
(30) Fuchs, T. M.; Hoffmann, R. C.; Niesen, T. P.; Tew, H.; Bill, J.; Aldinger, F. *J. Mater. Chem.* **2002**, *12*, 1597.

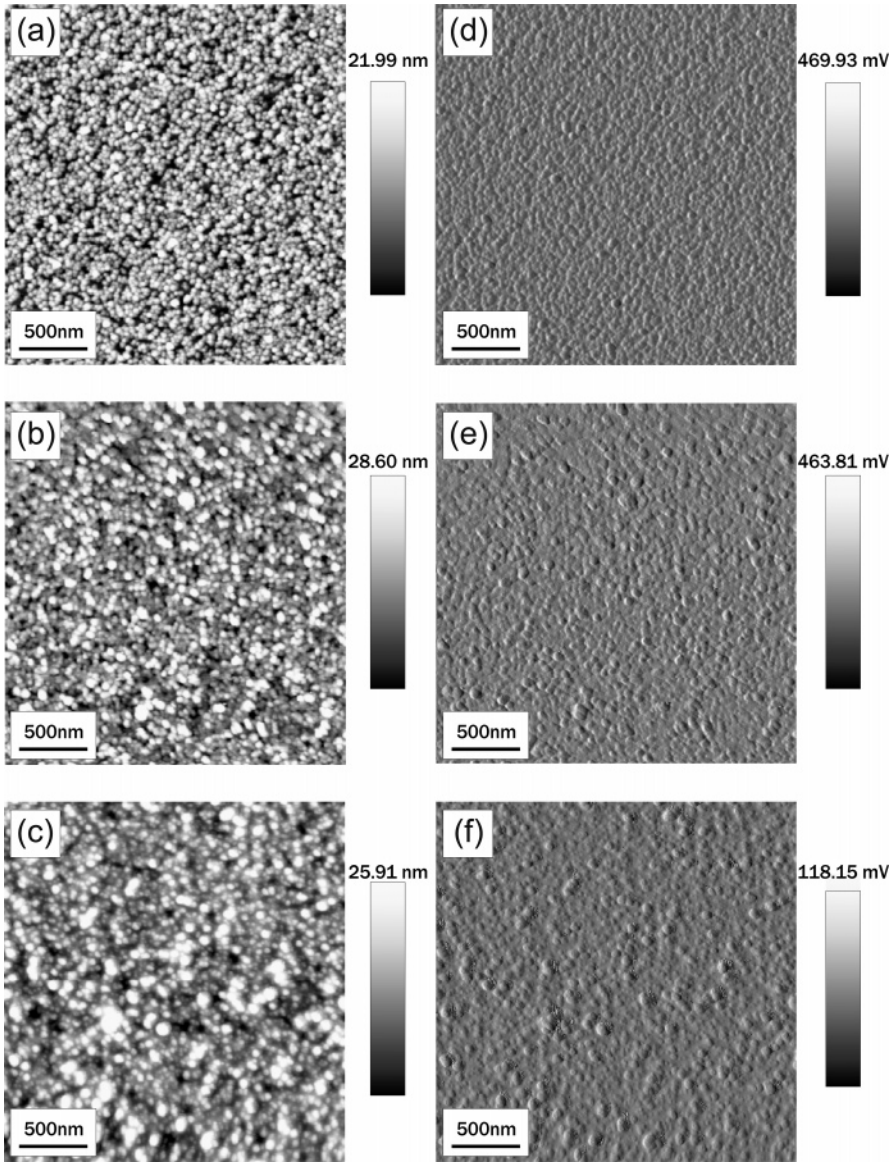

Figure 7. AFM topographic images of films from solutions containing 15 mM Ti, 30 mM H_2O_2, 5 mM V, and 100 mM HCl after (a) 1 h, (b) 2 h, and (c) 3 h, respectively, and corresponding deflection mode images (d), (e), and (f), respectively.

the first stages of the film growth (Figure 7) only a slight increase of the surface roughness with the thickness could be observed (Figure 9b). This behavior was observed earlier in other CBD reactions.[31]

XPS analysis was applied to determine the Ti and V content in the subsurface region of the oxide film after various reactions times (Figure 10). It followed that both Ti and V are incorporated within the developing oxide film upon deposition; besides no indication of chlorine was found in the films. A constrained curve fitting of the Ti 2p and V 2p spin−orbit doublet (i.e., taking the same Gauss-Lorentz fractions and a fixed area ratio of 0.5 for the $2p_{3/2}$ and $2p_{1/2}$ main peaks in the concerned spin−orbit doublets) was performed to the measured XPS spectra after subtraction of the Shirley-type background (to remove the background of inelastically scattered photoelectrons). It followed that the Ti $2p_{3/2}$ and Ti $2p_{1/2}$ main peaks could each be accurately described with only one oxidic main peak positioned at a binding energy (BE) of 464.5 ± 0.1 and 458.9 ± 0.1 eV, respectively (Table 2). The BEs of the resolved Ti $2p_{3/2}$ and Ti $2p_{1/2}$ main peaks, as well as the associated value for the spin−orbit splitting of the Ti 2p doublet, are in agreement with corresponding literature values[32,33] for TiO_2 (Figure 10a, Table 2). Apparently, the chemical shift of the Ti $2p_{3/2}$ main peak for Ti in a solid solution of $(Ti_{1-x}V_x)O_2$ with respect to Ti in a TiO_2 reference is too small to be resolved using XPS.[33] The corresponding V $2p_{3/2}$ and V $2p_{1/2}$ main peaks, on the other hand, are each constituted of two spectral contributions (Figure 10b, Table 3), as attributed to vanadium ions in the +V (the higher BE side contributions at 517.5 ± 0.1 and 524.7 ± 0.1 eV, respectively) and the +IV valence state (the lower BE side contributions at 516.3 ± 0.1 and 523.4 ± 0.1 eV, respectively).[33,34] Finally, the corresponding O 1s spectra could be accurately described with two spectral

(31) Gao, Y.; Masuda, Y.; Koumoto, K. *Chem. Mater.* **2003**, *15*, 2399.
(32) Dupin, J. C.; Gonbeau, D.; Vinatier, P.; Levasseur, A. *Phys. Chem. Chem. Phys.* **2000**, *2*, 1319.
(33) Chiarello, G.; Robba, D.; De Michele, G.; Parmigiani, F. *Appl. Surf. Sci.* **1993**, *64*, 91.
(34) Silversmit, G.; Depla, D.; Poelman, H.; Marin, G. B.; De Gryse, R. *J. Electron. Spectrosc. Relat. Phenom.* **2004**, *135*, 167.

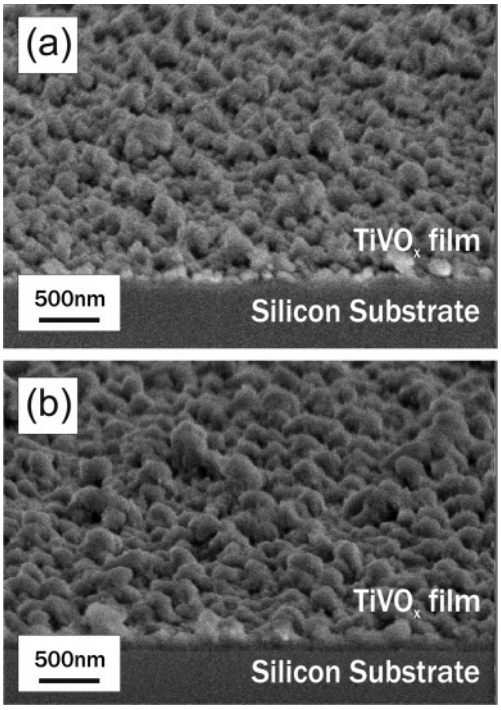

Figure 8. SEM micrographs of cross sections of films from solutions containing 15 mM Ti, 30 mM H_2O_2, 5 mM V, and 100 mM HCl after (a) 2 × 2 h and (b) 3 × 2 h, respectively.

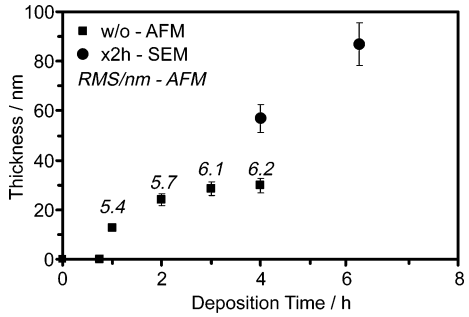

Figure 9. (a) Comparison of the film thickness as a function of deposition time for solution containing 15 mM Ti, 30 mM H_2O_2, 5 mM V, and 100 mM HCl for different renewal rates; without renewal (squares; determined by AFM) and every 2 h (circles; determined by SEM). Corresponding RMS values are included in italics.

contributions (Table 3), as attributed to oxygen ions in the "bulk" oxide [i.e., the $(Ti_{1-x}V_x)O_2$ solid solution; the lower BE side contribution at 530.4 ± 0.1 eV] and at the hydroxylated oxide surface (i.e., the higher BE side contribution at 531.9 ± 0.1 eV). As indicated by the quantitative analysis of the resolved Ti $2p_{3/2}$, V $2p_{3/2}$ and O 1s peak intensities, the atomic ratios of both Ti:V and Ti:(+V):(+IV) within the grown oxide films do not vary drastically with increasing deposition time (Table 4). With increasing reaction time, the newly formed oxide at the reacting film surface becomes slightly richer in Ti (i.e., the Ti:V ratio increases; Table 4). However, the relative Ti content in the grown oxide films always remained below the corresponding Ti content in the precipitates in powder form, as obtained from the same reaction solution (compare Tables 4 and 1).

Conclusions

The focus of the current investigations was put on the elucidation of the deposition mechanism rather than optimizing the titania/vanadium oxide films with respect to thickness and surface roughness. The work presented here demonstrates that a combination of DLS and UV/Vis spectroscopy is a suitable tool to understand the processes in the reaction solution of CBD for the synthesis of mixed titania/vanadium oxide films. These methods are easily applicable and commercial instruments exist also for in situ investigations. Whereas DLS elucidates particle and agglomerate formation, UV/Vis spectroscopy adds information about the chemical nature of the species in solution. When the findings obtained with these methods are combined with the results of XRD and XPS investigations of films grown from the beforementioned solutions, a scheme can now be proposed, which correlates events in the reaction solution with the film formation process on the substrate (Figure 11).

The UV/Vis investigations of the reaction solutions showed that titania or titanium-rich particles are formed first, whereas more vanadium-rich phases are generated after a

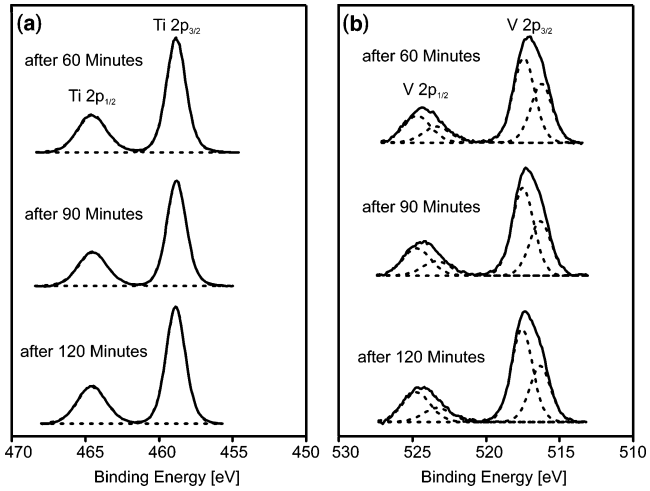

Figure 10. XPS spectra of films grown on silicon substrates from solutions containing 15 mM Ti, 30 mM H_2O_2, 100 mM HCl, and 5 mM V after 1, 1.5, and 2 h. Resolved (a) Ti 2p main peaks and (b) V 2p main peaks, as obtained by constrained peak fitting.

Table 2. XPS Results (Binding Energies in eV) of Samples (15 mM Ti, 5 mM V, and 100 mM HCl) Grown with Different Deposition Times for Ti 2p Peaks as Well as Binding Energy Differences (ΔBE)

sample	Ti $2p_{3/2}$	Ti $2p_{1/2}$	ΔBE (Ti $2p_{3/2}$ – Ti $2p_{1/2}$)
after 60 min	458.8	464.5	5.7
after 90 min	458.8	464.6	5.8
after 120 min	458.9	464.6	5.7

Table 3. XPS Results (Binding Energies in eV) of Samples (15 mM Ti, 5 mM V, and 100 mM HCl) Grown with Different Deposition Times Showing the Contributions to the V 2p Peaks as Well as the Corresponding Binding Energy Differences (ΔBE) and Contributions to the O 1s Peak

sample	V $2p_{3/2}$	V $2p_{1/2}$	ΔBE (V $2p_{3/2}$ – V $2p_{1/2}$)	O 1s
after 60 min	517.5, 516.3	524.7, 523.4	7.2, 7.1	531.9, 530.4
after 90 min	517.5, 516.3	524.7, 523.4	7.2, 7.1	531.9, 530.4
after 120 min	517.6, 516.3	524.7, 523.3	7.1, 7.0	532.0, 530.5

Table 4. Ratio of Ti:V and Ti:(+V):(+IV) According to XPS Curve Fits

sample	Ti:V	Ti:(+V):(+IV)
after 60 min	2.5:1.0	6.2:1.5:1.0
after 90 min	2.7:1.0	6.8:1.5:1.0
after 120 min	2.7:1.0	7.3:1.7:1.0

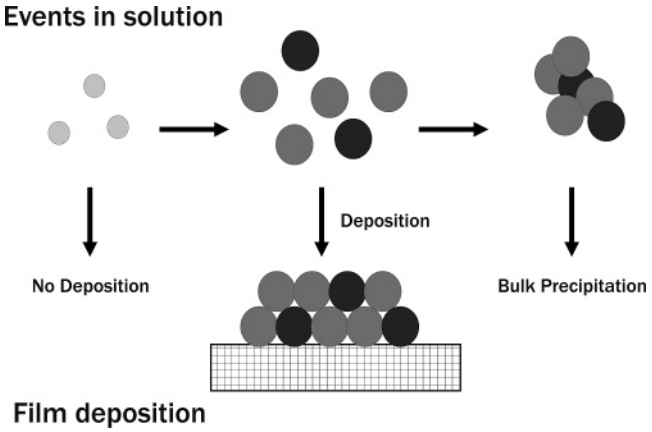

Figure 11. Schematic illustration of the different stages of particle/agglomerate formation in solution and film deposition: Multicomponent system TiO_2/VO_x.

certain period of time. DLS measurements (in addition to XRD) on the other hand reveal the formation of nanosized particles, which after a certain induction time agglomerate rapidly. The points in time, when the changes in UV/Vis and DLS occur, coincide. In other words, within the induction time titania or titanium-rich particles exist as stable suspensions, whereas with the formation of more vanadium-rich phases rapid agglomeration occurs.

SEM and AFM investigations show that not all particle sizes are suitable for the film growth. During the beforementioned induction time, no film formation is observed. Films are exclusively built up in a later stage, i.e., when the nanoscalic particles have reached a suitable size. Larger agglomerates do not contribute to the film growth either, but rather sediment on the surface in the form of defects. Consequently, the produced films exhibit only a small (or no) compositional gradient, which is revealed by XPS. As a consequence of this formation mechanism, the reaction system investigated here might rather be suitable for the deposition of compositions richer in titanium than in vanadium.

Acknowledgment. Dedicated to Prof. G. Petzow on the occasion of his 80th birthday. We thank Mr. Daniel Kohl for help with the experimental work.

CM060301T